# Appendix A

# Average Kinetic Energy Release in Sequential Fragmentation

In this appendix, a calculation is made for the expected average velocity following sequential $C_2$ loss. By calculating the kinetic energy release for each fragmentation process, it is possible to model the experimental spatial distributions. The crux of this calculation hangs on the fact that the final internal energy is independent of size.

The average kinetic energy release $\langle KER \rangle^{cm}$ can be defined as Eq. A.1 [Eng86, Eng87] [1].

$$\langle KER \rangle^{cm} = 2 * \frac{E_{int} - E_a}{s - 1} \tag{A.1}$$

where $E_{int}$ is the initial internal energy, $E_a$ is the activation energy, and $s$ is the number of degrees of freedom. When no reverse activation barrier is present, as indicated by measurements on $C_{60}$ [RHR90], the activation energy is equal to the dissociation energy. The first fragmentation process can be written as

$$\langle KER \rangle^{cm} = 2 * \frac{E_{int_1} - D_1}{s_1 - 1} \tag{A.2}$$

where the index 1 indicates the first fragmentation step. The next step in the sequential fragmentation process is shown in Eq. A.3

[1] A superscript of 'cm' denotes the KER is calculated in the center of mass frame, while lab indicates that the KER is in the laboratory frame

$$\langle KER_2\rangle^{cm} = 2 * \frac{E_{int_2} - D_2}{s_2 - 1} \tag{A.3}$$

where $E_{int_2}$ = $E_{int}$ - $D_1$ - $E_{frag}$ - $\langle KER_1\rangle$, i.e., the amount of energy lost by the first fragmentation process.

$$\langle KER_2\rangle^{cm} = 2 * \frac{E_{int_1} - D_2 - E_{frag} - \langle KER_1\rangle}{s_2 - 1} \tag{A.4}$$

The energy content of the fragment, $E_{frag}$, and the first KER, $\langle KER_1\rangle$, are assumed to be much smaller than $D_1$ energy for this calculation. The KER in Eq. A.3 and Eq. A.4 are in the center of mass frame. For comparison to experiment, a transformation from the center of mass frame to the laboratory frame will be made. Here, it will be indicated as the proportionality constant $B_{\Delta N}$, where $\Delta N$ denotes the number of fragmentation step. The total KER after two fragmentation steps can be written as

$$\begin{aligned} \langle KER_{total}\rangle_2^{lab} &= B_1\langle KER_1\rangle^{cm} + B_2\langle KER_2\rangle^{cm} \\ &= 2 * B_1\frac{(E_{int} - D_1)}{s_1 - 1} + 2 * B_2\frac{(E_{int} - D_1 - D_2)}{s_2 - 1} \end{aligned} \tag{A.5}$$

The third fragmentation step results in

$$\begin{aligned} \langle KER_{total}\rangle_3^{lab} &= B_1\langle KER_1\rangle^{cm} + B_2\langle KER_2\rangle^{cm} + B_3\langle KER_3\rangle^{cm} \\ &= 2 * B_1\frac{(E_{int} - D_1)}{s_1 - 1} + 2 * B_2\frac{(E_{int} - D_1 - D_2)}{s_2 - 1} \\ &+ 2 * B_3\frac{(E_{int} - D_1 - D_2 - D_3)}{s_3 - 1} \end{aligned} \tag{A.6}$$

The degrees of freedom, $s_{\Delta N}$, can be written as $s_{\Delta N} = 3 * (M - K(\Delta N - 1)) - 6 = (3M - 6) - 3K(\Delta N - 1)$, where M is the original number of atoms, K is the number of atoms lost per fragmentation step (which strictly requires an index, but for the present it will be assumed that the fragment size is equivalent for each step).

$$\langle KER_{total}\rangle^{lab} = \sum_{\Delta N=1}^{\Delta N} 2 * B_{\Delta N}\frac{E_{int} - \sum_{\Delta N'=1}^{\Delta N} D_{\Delta N'}}{(3M - 7) - 3K(\Delta N - 1)} \tag{A.7}$$

This equation can be applied to $C_{60}$, where M=60 and K=2, thus $s_{\Delta N} = s_{60-2\Delta N} = 3 * (60 - 2(\Delta N - 1)) - 6 = 174 - 6(\Delta N - 1)$, resulting in

$$\langle KER_{total}\rangle^{lab} = \sum_{\Delta N=1}^{\Delta N} 2 * B_{\Delta N}\frac{E_{int} - \sum_{\Delta N'=1}^{\Delta N} D_{60-2\Delta N'}}{173 - 6(\Delta N - 1)} \tag{A.8}$$

However since the initial internal energy, $E_{int}$ is not known, a trick can be used so that a final internal energy, $E_{int_{final}}$ is considered and for each fragmentation step the energy loss associated with that fragmentation is added to the internal energy. The internal energy of the fragment prior to the fragmentation can be written as

$$E_{int_{final}} = E_{int} - D \Rightarrow E_{int} = E_{int_{final}} + D \tag{A.9}$$

Following similar calculations, as from Eq. A.2 to Eq. A.8, a similar equation results.

$$\langle KER_{total} \rangle^{lab} = \sum_{\Delta N=1}^{\Delta N} 2 * B_{\Delta N} \frac{E_{int_{final}} + \sum_{\Delta N'=1}^{\Delta N} D_{60-2\Delta N'}}{173 - 6(\Delta N - 1)} \tag{A.10}$$

The final energy, $E_{int_{final}}$, is considered to be the same for each fragment, regardless of mass, and this energy leads to no further fragmentation on the time scale shorter that the time of flight.

$B_{\Delta N}$ is the conversion factor between the center of mass and laboratory frame. The KER is determined from the sum of the kinetic energy of the two particles involved in the fragmentation.

$$KER = \frac{1}{2} m_r v_r^2 = \frac{1}{2} m_1 v_1^2 + \frac{1}{2} m_2 v_2^2 \tag{A.11}$$

where $m_r$ is the reduced mass and $v_r$ is the relative velocity in the center of mass frame. We want to determine the factor between $v_r$ and the velocity of one of the fragments, $v_1$. The velocity, $v_1$ can be determined by conservation of momentum, $m_1 v_1$ = - $m_2 v_2$. Solving for $v_2$ and plugging into Eq. A.11 results in Eq. A.12.

$$\frac{1}{2} m_r v_r^2 = \frac{1}{2} m_1 v_1^2 + \frac{1}{2} m_2 \left( \frac{m_1}{m_2} v_1 \right)^2 \tag{A.12}$$

solving for $v_r$,

$$v_r^2 = v_1^2 * \left( \frac{(m_1 + m_2)}{m_2} \right)^2 \tag{A.13}$$

and plugging this into Eq. A.11,

$$\begin{aligned}
\langle KER\rangle^{cm} &= \frac{1}{2}m_r v_r^2 \\
&= \frac{1}{2}m_r v_1^2 * \left(\frac{(m_1+m_2)}{m_2}\right)^2 \\
&= \frac{1}{2}\frac{m_1 m_2}{m_1+m_2}\left(\frac{(m_1+m_2)}{m_2}\right)^2 v_1^2 \\
\langle KER\rangle^{cm} &= \frac{m_1+m_2}{m_2}\langle KER\rangle^{lab} \qquad \text{(A.14)}
\end{aligned}$$

Thus, $B = \frac{m_2}{(m_1+m_2)}$, where $m_2$ is the mass of $C_2$ and $m_1$ is the mass of the larger fragment. The values of B are indicated for several fragments in Table A.1. This is put into Eq. A.10:

$$\langle KER_{total}\rangle^{lab} = \sum_{\Delta N=1}^{\Delta N} 2 * \frac{m_2}{m_{60-2\Delta N}+m_2}\frac{E_{int_{final}} + \sum_{\Delta N'=1}^{\Delta N} D_{60-2\Delta N'}}{173-6(\Delta N-1)} \qquad \text{(A.15)}$$

The known dissociation energies and number of degrees of freedom of the different fragmentation steps of $C_{60}$ (see Table A.1) can be inserted into Eq. A.10 to calculate the accumulated KER.

Table A.1: *Dissociation energies and number of modes for different fragmentation steps. Dissociation energy values are from [TAG01].*

| $\Delta N$ | Notation | $D_{60-2(\Delta N-1)}$ [eV] | Degrees of freedom | B |
|---|---|---|---|---|
| 1 | $C_{60}^{+} \rightarrow C_{58}^{+}$ | 9.75 | 174 | 1/30 |
| 2 | $C_{58}^{+} \rightarrow C_{56}^{+}$ | 8.25 | 168 | 1/29 |
| 3 | $C_{56}^{+} \rightarrow C_{54}^{+}$ | 8.65 | 162 | 1/28 |
| 4 | $C_{54}^{+} \rightarrow C_{52}^{+}$ | 8.4 | 156 | 1/27 |
| 5 | $C_{52}^{+} \rightarrow C_{50}^{+}$ | 8.4 | 150 | 1/26 |
| 6 | $C_{50}^{+} \rightarrow C_{48}^{+}$ | 8.75 | 144 | 1/25 |
| 7 | $C_{48}^{+} \rightarrow C_{46}^{+}$ | 8.3 | 138 | 1/24 |
| 8 | $C_{46}^{+} \rightarrow C_{44}^{+}$ | 8.0 | 132 | 1/23 |
| average | | 8.6 | 153 | 1/26.5 |

Table A.2: *Calculation of accumulated KER in laboratory and center of mass frame. Laboratory frame KER calculated from Eq. A.15 and values from Table A.1, with* $E_{int_{final}} = 40eV$. *The center of mass KER is calculated by* $1/B * \langle KER \rangle^{lab}$.

| $\Delta N$ | Notation | $\langle KER_{total} \rangle^{lab}[meV]$ | $\langle KER_{total} \rangle^{cm}[eV]$ |
|---|---|---|---|
| 1 | $C_{60}^{+} \rightarrow C_{58}^{+}$ | 19.17 | 0.58 |
| 2 | $C_{58}^{+} \rightarrow C_{56}^{+}$ | 43.12 | 1.25 |
| 3 | $C_{56}^{+} \rightarrow C_{54}^{+}$ | 72.63 | 2.03 |
| 4 | $C_{54}^{+} \rightarrow C_{52}^{+}$ | 108.56 | 2.93 |
| 5 | $C_{52}^{+} \rightarrow C_{50}^{+}$ | 151.64 | 3.94 |
| 6 | $C_{50}^{+} \rightarrow C_{48}^{+}$ | 203.22 | 5.08 |
| 7 | $C_{48}^{+} \rightarrow C_{46}^{+}$ | 264.32 | 6.34 |
| 8 | $C_{46}^{+} \rightarrow C_{44}^{+}$ | 336.31 | 7.74 |

**Simplification to one fit parameter**

To simplify Eq. A.10, a few average values will be used. First, the average value of s after a certain number of fragmentation steps, can be determined by $\widetilde{s} = (\sum_{i=1}^{\Delta N} s_i)/\Delta N$. This approximation is justified because the number of modes changes slowly in comparison to the change in internal energy. For 8 fragmentation steps, $\widetilde{s} = 153$. The second approximation is to take the average dissociation energy. Defined in a similar way as the average number of degrees of freedom, $\widetilde{D} = (\sum_{i=1}^{\Delta N} D_i)/\Delta N$. For 8 fragmentation steps, $\widetilde{D} = 8.4$. The final approximation is the average B, which is equivalent to taking an average fragment size. $\widetilde{B} = (\sum_{i=1}^{\Delta N} B_i)/\Delta N$. For 8 fragmentation steps, $\widetilde{B}$=1/26.5.

Substituting these into Eq. A.10 gives

$$\begin{aligned} \langle KER_{total} \rangle^{lab} &= \sum_{\Delta N=1}^{\Delta N} 2 * \widetilde{B} \frac{E_{int_{final}} + \Delta N * \widetilde{D}}{\widetilde{s}} \\ &= \frac{2 * \widetilde{B}}{\widetilde{s}} \sum \left( E_{int_{final}} + \Delta N * \widetilde{D} \right) \end{aligned} \tag{A.16}$$

The first few steps are shown below

$$\begin{aligned} \langle KER_{total} \rangle_1^{lab} &= \frac{2 * \widetilde{B}}{\widetilde{s}} (E_{int_{final}} + 1 * \widetilde{D}) \\ \langle KER_{total} \rangle_2^{lab} &= \frac{2 * \widetilde{B}}{\widetilde{s}} (2 * E_{int_{final}} + 3 * \widetilde{D}) \\ \langle KER_{total} \rangle_3^{lab} &= \frac{2 * \widetilde{B}}{\widetilde{s}} (3 * E_{int_{final}} + 6 * \widetilde{D}) \end{aligned} \tag{A.17}$$

This can be simplified to the Eq. A.19, which is a function which is solely dependent on the number of $C_2$ units.

$$\begin{aligned} \langle KER_{total} \rangle_{\Delta N}^{lab} &= 2 * \widetilde{B} \frac{\Delta N * E_{int_{final}} + 1/2 * \Delta N(\Delta N + 1) * \widetilde{D}}{\widetilde{s}} \\ &= 2 * \widetilde{B} \frac{(E_{int_{final}} + \frac{1}{2}\widetilde{D})\Delta N + \frac{1}{2}\widetilde{D}(\Delta N)^2}{\widetilde{s}} \end{aligned} \tag{A.18}$$

For $C_{60}$, the following numbers have been used. $E_{int_{final}}$ is the internal energy which provides a rate of fragmentation longer than the time of flight, which is about 40 eV. This is assumed to be independent of final size. The average number of degrees of

freedom, $\widetilde{s}$, is set to 153, the average $\widetilde{B}$ is set to 1/26.5, and the average dissociation energy, $\widetilde{D}$, is taken to be 8.6 eV.

$$\begin{aligned}
\langle KER_{total}\rangle_{\Delta N}^{lab} &= \frac{2*\widetilde{B}}{\widetilde{s}}\left((E_{int_{final}}+\frac{1}{2}\widetilde{D})\Delta N+\frac{1}{2}\widetilde{D}(\Delta N)^2\right) \\
&= \frac{2*1/26.5}{153}*\left((40+\frac{1}{2}8.6)\Delta N+\frac{1}{2}8.6(\Delta N)^2\right) \\
&= \frac{2*1/26.5}{153}*\left((40+4.28)\Delta N+4.28*(\Delta N)^2\right) \\
&= \frac{2*1/26.5}{153}*4.28*(10.3\Delta N+(\Delta N)^2) \\
&= 2.11*10^{-3}*(10.3\Delta N+(\Delta N)^2) \qquad \text{(A.19)}
\end{aligned}$$

Defining the constant A $\equiv 2.11*10^{-3}$, the final equation is Eq. A.20.

$$\langle KER_{total}\rangle_{\Delta N}^{lab} = A*(10.3\Delta N+(\Delta N)^2) \qquad \text{(A.20)}$$

.

Table A.3: *This table is similar to Table A.2, except here the values are from Eq. A.20 taking several approximations into account. Laboratory frame KER calculated from Eq. A.20 and values from Table A.1, with* $E_{int_{final}} = 40eV$. *The center of mass KER is calculated by* $1/B * \langle KER \rangle^{lab}$.

| $\Delta N$ | Fragmentation | $\langle KER_{total} \rangle^{lab}$ [meV] | $\langle KER_{total} \rangle^{cm}$ [eV] |
|---|---|---|---|
| 1 | $C_{60}^{+} \rightarrow C_{58}^{+}$ | 23.8 | 0.72 |
| 2 | $C_{58}^{+} \rightarrow C_{56}^{+}$ | 51.9 | 1.51 |
| 3 | $C_{56}^{+} \rightarrow C_{54}^{+}$ | 84.2 | 2.36 |
| 4 | $C_{54}^{+} \rightarrow C_{52}^{+}$ | 120.7 | 3.26 |
| 5 | $C_{52}^{+} \rightarrow C_{50}^{+}$ | 161.4 | 4.20 |
| 6 | $C_{50}^{+} \rightarrow C_{48}^{+}$ | 206.4 | 5.16 |
| 7 | $C_{48}^{+} \rightarrow C_{46}^{+}$ | 255.5 | 6.13 |
| 8 | $C_{46}^{+} \rightarrow C_{44}^{+}$ | 308.9 | 7.10 |

# Appendix B

# Spatially Resolved Detection : From Pixels to $\langle KER \rangle^{cm}$

In this appendix, the data evaluation of the position sensitive detector is explained. The X, Y, and time of flight coordinates are recorded for each event.

### Projections

Fragmentation produces a three dimensional spatial distribution. It is assumed to be isotropic and Gaussian in each dimension for $C_{60}$.

$$f(v_i)dv_i \propto e^{-v_i^2 m_r/2k_BT}dv_i \tag{B.1}$$

for i= x,y, and z. $f(v_i)$ is the velocity distribution in one direction. The total velocity distribution is given by

$$\begin{aligned} f(v_x, v_y, v_z)dv_x dv_y dv_z &\propto e^{-v_x^2 m_r/2k_BT} e^{-v_y^2 m_r/2k_BT} e^{-v_z^2 m_r/2k_BT} dv_x dv_y dv_z \\ &\propto e^{-\left(v_x^2+v_y^2+v_z^2\right)m_r/2k_BT} \end{aligned} \tag{B.2}$$

The three dimensional distribution is integrated over the z component to give the two dimensional image.

$$\begin{aligned}\int f(v_x, v_y, v_z)dv_z &\propto \int e^{-v_x^2 m_r/2k_BT} e^{-v_y^2 m_r/2k_BT} e^{-v_z^2 m_r/2k_BT} dv_z \\ &\propto e^{-\left(v_x^2+v_y^2\right)m_r/2k_BT} \int e^{-v_z^2 m_r/2k_BT} dv_z \\ &\propto K e^{-\left(v_x^2+v_y^2\right)m_r/2k_BT} \end{aligned} \tag{B.3}$$

where K is equal to the integral and a constant.

The 2D image is then projected onto the x or y axis. This is achieved by integration over y or x, respectively.

$$\begin{aligned}\int f(v_x, v_y)dv_y &\propto \int K e^{-v_x^2 m_r/2k_BT} e^{-v_y^2 m_r/2k_BT} \\ &\propto K e^{-\left(v_x^2\right)m_r/2k_BT} \int e^{-v_y^2 m_r/2k_BT} dv_y \\ &\propto K' e^{-\left(v_x^2\right)m_r/2k_BT} \end{aligned} \tag{B.4}$$

where K' is equal to the integral of the y component and a constant. The velocity distribution in the center of mass can be converted to the lab frame of one of the fragments. The KER is determined from the sum of the kinetic energy of the two particles involved in the fragmentation.

$$KER = \frac{1}{2} m_r v_r^2 = \frac{1}{2} m_1 v_1^2 + \frac{1}{2} m_2 v_2^2 \tag{B.5}$$

where $m_r$ is the reduced mass and $v_r$ is the relative velocity in the center of mass frame. We want to determine the factor between $v_r$ and the velocity of one of the fragments, $v_1$. The velocity, $v_1$ can be determined by conservation of momentum, $m_1 v_1$ = - $m_2 v_2$. Solving for $v_2$ and plugging into Eq. A.11 results in Eq. A.12.

$$\frac{1}{2} m_r v_r^2 = \frac{1}{2} m_1 v_1^2 + \frac{1}{2} m_2 \left(\frac{m_1}{m_2} v_1\right)^2 \tag{B.6}$$

solving for $v_r$,

$$v_r^2 = v_1^2 * \left(\frac{(m_1 + m_2)}{m_2}\right)^2 \tag{B.7}$$

Thus the final equation of Eq. B.4, can be rewritten as

$$f(v_{1_x}) = K' e^{-\left(v_{1_x}^2\right)m_1/2k_BT} \tag{B.8}$$

The projections are fit with a Gaussian, which can be defined as

$$f(p) = e^{-v_{1_x}^2/2\sigma^2} \tag{B.9}$$

where $v_{1_x}$ indicates the velocity of particle one in the x direction. The velocity at 1/e can be easily determined by

$$\begin{aligned} e^{-v^2/2\sigma^2} &= e^{-m_{60-2\Delta N}v_{60-2\Delta N}^2/2k_BT} \\ \frac{1}{2\sigma^2} &= \frac{m_{60-2\Delta N}}{2k_BT} \\ \Rightarrow \sigma &= \sqrt{\frac{k_BT}{m_{60-2\Delta N}}} \end{aligned} \tag{B.10}$$

The raw measured width is the convolution of the previous 2D image and the additional width gained upon fragmentation.

A special property of Gaussian distributions is that the convolution of two Gaussians results in a third Gaussian whose width is determined by the squares of the widths.

$$\sigma_{AB}^2 = \sigma_A^2 + \sigma_B^2 \tag{B.11}$$

Either the width of the previous 2D image can be deconvoluted or the width of $C_{60}^{n+}$. It is essential to take this deconvolution in velocity space.

### Pixels to Velocity

The distance in pixels can be converted to velocity by the relation

$$v_i = \frac{d_i}{t_{C_n}} \tag{B.12}$$

where $i$ indicates either the x or y axis (refer to Fig. 2.22 for orientation of the axes). The time of flight of mass $C_n$, $t_{C_n}$, is given by the relation

$$t_{c_n} = \frac{L}{v_{z_{total}}} \tag{B.13}$$

where $L$ is the length of the time of flight mass spectrometer and $v_{z_{total}} = v_{acc} + v_z$, the velocity due to the acceleration zone and the initial velocity in the z direction.

The acceleration velocity, $v_{acc}$ is dependent on the the charge, $Ze_0$, electric potential of the acceleration region, $V$, and mass, $m$, as is shown in Eq. C.5.

$$v_{acc} = \sqrt{\frac{2Ze_0V}{m}} \tag{B.14}$$

The velocity due to fragmentation, $v_z$, is negligible in comparison to $v_{acc}$. Thus, the lateral velocity (perpendicular to time of flight axis) for x and y can be written as

$$v_i = \frac{d_p * N * \sqrt{\frac{2Ze_0V}{m}}}{L} \tag{B.15}$$

where $d_p$ is the width of the pixel, which is known geometrically to be 0.25 mm/pixels and $N$ is the number of pixels, the measured quantity. For a given voltage, this expression can be reduced to

$$v_i = b * N * \sqrt{\frac{Ze_0}{m}} \tag{B.16}$$

where b is a constant of the experiment. In sections "kinetic energy release distribution: $C_{60} \rightarrow C_{58}$" and "Fragmentation by sequential $C_2$ loss", the voltage spanning across the 2 cm interaction region was 500 V (with excitation occurring in the center), which leads to a $b$ value of

$$b = \frac{(d_p * \sqrt{2V}}{L} = \frac{0.25 * 10^{-3}[m/pixel] * \sqrt{2 * 250[V]}}{0.45[m]} = 0.012423[\sqrt{V}/pixels] \tag{B.17}$$

A second voltage which is used for results presented in this thesis (Section Deviations from a single gaussian projection") was 1000 V. The corresponding $b$ value is

$$b = \frac{d_p * \sqrt{2V}}{L} = \frac{0.25 * 10^{-3}[m/pixel] * \sqrt{2 * 500[V]}}{0.45[m]} = 0.017568[\sqrt{V}/pixels] \tag{B.18}$$

**Velocity to KER**

The measured width of a projection is directly proportional to the velocity in that dimension. The component of velocity is part of the total velocity, however it is found that the width of the Gaussian fit in $v_x$ is the same as the width of v( Eq. B.2 to Eq. B.4). From Eq. B.11, there are two ways in which to interpret the data. The first is

$$\sigma^2_{60-\Delta N}(calc) = \sigma^2_{60-\Delta N}(meas) + \sigma^2_{60}(meas) \tag{B.19}$$

where ($meas$) indicates the fit experimental data and ($calc$) indicates the calculated true width. By subtracting only the width of $C_{60}$ from the measured width, one gets the accumulated width.

The second deconvolution is

$$\sigma^2_{60-\Delta N}(calc) = \sigma^2_{(60-\Delta N-1)}(meas) + \sigma^2_{60-\Delta N}(calc) \tag{B.20}$$

The measured width of the previous spot size is subtracted from the measured width of the fragment to give the KER for that particular fragmentation.

The kinetic energy at $\sigma$ is calculated by

$$KE = \frac{1}{2} m_{60-2\Delta N} \sigma^2_{60-2\Delta N}(calc) \tag{B.21}$$

The average kinetic energy in the laboratory frame is defined as

$$\overline{\epsilon_{lab}} = \frac{1}{2} m_{58} \overline{v^2} = \frac{1}{2} m_{58} \frac{\int_0^\infty v^2 v^2 e^{-mv^2/2k_BT} dv}{\int_0^\infty v^2 e^{-mv^2/2k_BT} dv} = \frac{3}{2} k_B T \tag{B.22}$$

To transfer the center of mass frame, the following procedure is followed. The $KER^{cm}$ is determined from the sum of the kinetic energy of the two particles involved in the fragmentation.

$$KER^{cm} = \frac{1}{2} m_r v_r^2 = \frac{1}{2} m_1 v_1^2 + \frac{1}{2} m_2 v_2^2 \tag{B.23}$$

where $m_r$ is the reduced mass and $v_r$ is the relative velocity in the center of mass frame. We want to write $\langle KER \rangle$ as a function of velocity of one of the fragments, e.g., $v_1$. The velocity, $v_1$ can be determined by conservation of momentum, $m_1 v_1 = - m_2 v_2$. Solving for $v_2$ and plugging into Eq. B.23 results in Eq. B.24.

$$\frac{1}{2} m_r v_r^2 = \frac{1}{2} m_1 v_1^2 + \frac{1}{2} m_2 \left( \frac{m_1}{m_2} v_1 \right)^2 \tag{B.24}$$

solving for $v_r$

$$v_r^2 = v_1^2 * \left( \frac{(m_1 + m_2)}{m_2} \right)^2 \tag{B.25}$$

which can be inserted into Eq. B.23.

$$\begin{aligned}
\langle KER \rangle^{cm} &= \frac{1}{2} m_r v_r^2 \\
&= \frac{1}{2} m_r \left( v_1 * \frac{(m_1 + m_2)}{m_2} \right)^2 \\
&= \frac{1}{2} \frac{m_1 m_2}{m_1 + m_2} \left( \frac{(m_1 + m_2)}{m_2} \right)^2 v_1^2 \\
&= \frac{m_1 + m_2}{m_2} \langle KER \rangle_1^{lab} \qquad \text{(B.26)}
\end{aligned}$$

# Appendix C

# Collection Probability of Particles for Different Kinetic Energies

The collection probability of a particle is dependent on the initial kinetic energy (KE). When the velocity components perpendicular to the time of flight (TOF) axis are too large, then the particle will not be incident onto the detector. In this short calculation, we seek to find the percentage of particles to hit the detector for a given KE.

First, let us consider the case where the kinetic energy is well defined, $E_0$ and isotropic, producing a spherical shell with radius $R$, as is shown in Fig. C.1, at the detector. We want to integrate over $d\theta$ and $d\phi$. This is shown by the integration in Eq. (C.1).

$$2\int_0^{2\pi}\int_0^{\pi/2} R^2 sin\theta d\theta d\phi = 4\pi R^2 \tag{C.1}$$

This results in the surface area of $4\pi R^2$. (n.B. integration over $dr$ will give the volume of a sphere) and this is the normalization factor to give the percentage of particles striking the detector.

We must now define the MCP detector area. The detector has a radius of r, as sketched on the right hand side of Fig. C.1. This will change the limit of integration for $\theta$. The new limit is defined by the radius of the detector, $r$, and the radius of the shell, $R$. ($\sin\theta = \frac{r}{R}$)

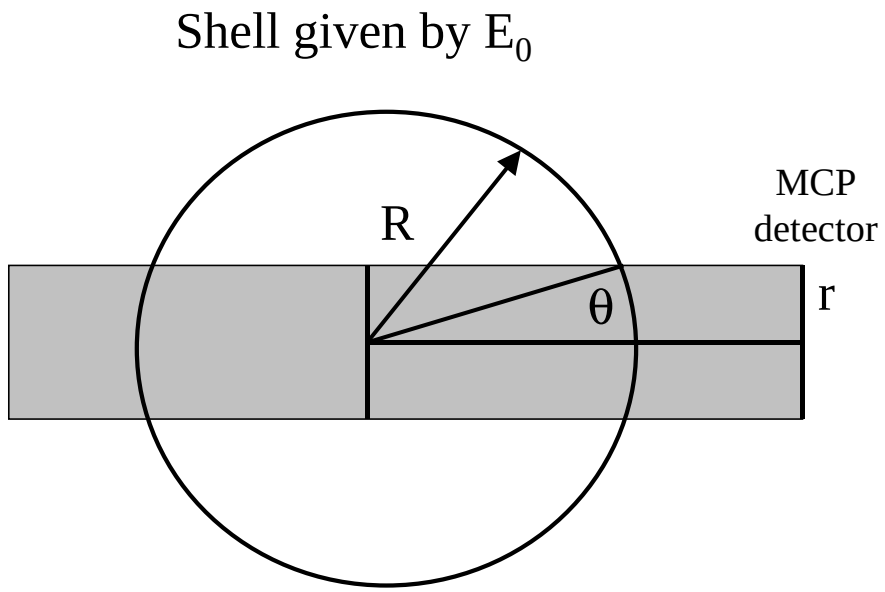


Figure C.1: *Schematic of calculation used to determine the collection probability*

$$2\int_0^{2\pi}\int_0^{arcsin(r/R)} R^2 sin\theta d\theta d\phi = 4\pi R^2 * \left[1 - \sqrt{1 - \left(\frac{r}{R}\right)^2}\right] \tag{C.2}$$

Thus the detection probability is given by

$$W = \left[1 - \sqrt{1 - \left(\frac{r}{R}\right)^2}\right] \tag{C.3}$$

This relation takes only geometric factors into account. $r$ is a fixed number at 25 mm. $R$ can be determined by multiplying the radial velocity, $v_r$, by the time-of-flight, $t$. This equation breaks down when $r < R$. When this occurs, all particles hit the detector.

The radial velocity, $v_r$, is related to the kinetic energy by the relation

$$v_r = \sqrt{\frac{2E_k}{m}} \tag{C.4}$$

where $E_k$ is the kinetic energy and $m$ is the mass.

The time-of-flight, $t$, is related to the length of the TOF spectrometer, $d_z$ and the velocity in the $z$ direction, $v_z$, which is determined by the relation

$$v_z = \sqrt{\frac{2ZU}{m}} \tag{C.5}$$

where $Z$ is the charge and $U$ is the potential. Here we assume that the acceleration velocity is much larger than the initial kinetic energy in the $z$ direction, thus $v_{z_0} =$ 0 m/s. A calculation including an initial velocity in $z$, $v_{z_0} = 1500$ m/s, changes the collection percentage by 0.53%.

Putting $\mathrm{v}_r$ and $t$ together, we arrive at

$$R = \sqrt{\frac{2E_k}{m}} * \frac{d_z}{\sqrt{\frac{2ZU}{m}}} = \sqrt{\frac{E_k}{ZU}} * d_z \tag{C.6}$$

Thus, the detection efficiency is NOT related to the mass, but rather the kinetic energy, charge, potential, and length of the time-of-flight apparatus. The potential is a constant, $z = 1$, $d_z = 2$ m, and $r = 0.025$ m. We can substitute everything into Eq. C.3.

$$W = \left[1 - \sqrt{1 - \left(\frac{r}{d_z\sqrt{\frac{E_k}{Z*U}}}\right)^2}\right] \tag{C.7}$$

The percentage of particles which will hit the detector for a certain kinetic energy is plotted in Fig. C.2. Here a comparison is made between the different detectors used in recent measurements. PSD denotes "position sensitive detector".

Note: the parameters for the PSD are different than for the linear TOF, namely $U = 250$ or 500 V, $r = 0.040$ m, and $d_z = 0.45$ m.

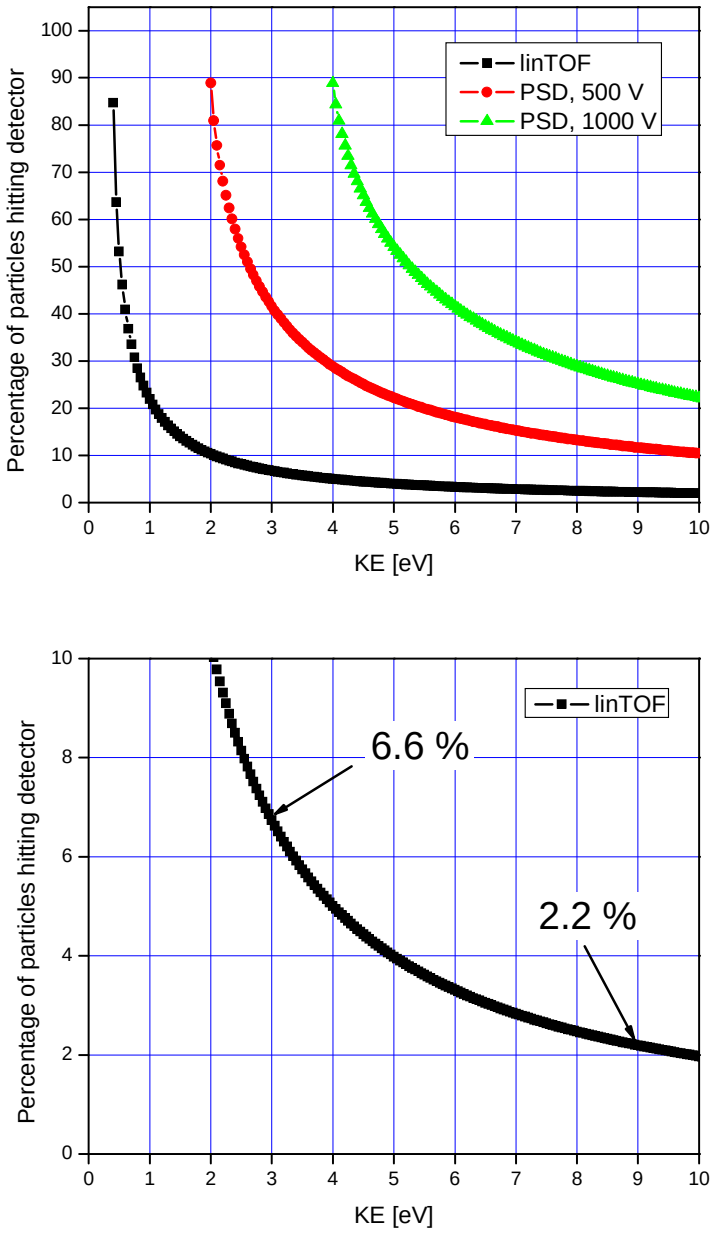


Figure C.2: *Particle collection probability for three different ion TOF configurations used in this work. The bottom graph shows a close up of the linear time of flight, indicating the percent of particles collected at 3 eV and 9 eV. These values correspond to the measured kinetic energy of $C^+$ fragments in a pump-probe measurement. These results are presented in Chapter 5.*

# Appendix D

# Magnetic Field Shielding

A charged particle moving in a magnetic field traverses a helical path as can be described by the Lorentz Force.

$$F = q(\overrightarrow{\mathcal{E}} + \overrightarrow{v} \times \overrightarrow{B}) \tag{D.1}$$

Due to their heavy mass and slow velocities, the magnetic force generally can be neglected for ions for typical TOF lengths (meters). Electrons (and light ions), however, will be strongly affected even by weak magnetic fields, such as the Earth's, which is approximately 50$\mu$T. Since the detection of particles is made within sub-mm (0.25 mm) resolution, sufficient shielding becomes critical.

To reduce the magnetic field in the chamber, concentric cylindrical mu-metal shields (Vacuum Schmelze GmbH) have been implemented. Mu-metal is a nickel-iron alloy (77% Ni, 14% Fe, 5% Cu and 4%Mo), which has a particularly high magnetic permeability. In theory, the most effective shielding is achieved through a geometric progression of successive surfaces [MDC89], e.g. the relation between inner and outer diameter. Practically, this is expensive and often only 2 or 3 cylinders provide enough shielding to reduce the magnetic fields at the center of the cylinders to a negligible level, a reduction of 8 orders of magnitude. For the present design, two cylinders were enough to sufficiently shield the Earth's magnetic field. The larger cylinder has an outer diameter of 148 mm (slightly smaller than the inner diameter of the vacuum cylinder). The smaller cylinder has an outer diameter of 100 mm. The thickness of both is 1 mm.

The attenuation factor of each individual cylinder can be calculated by the relation

[VAC88]:

$$A_i = \mu \cdot \frac{d_i}{D_i} \tag{D.2}$$

where $\mu$ is the magnetic permeability, $d_i$ is the thickness of the walls, and $D_i$ is the diameter of the cylinder. A typical value of magnetic permeability is 25000. The outer cylinder has an attenuation of 170 and the inner cylinder has an attenuation of 250. The attenuation factor for two concentric cylinders can be calculated with Eq. D.3.

$$S_{Total} = A_1 \cdot A_2 \cdot \left[1 - \left(\frac{D_2}{D_1}\right)\right] + A_1 + A_2 + 1 \tag{D.3}$$

The total magnetic shielding for the present apparatus is 1.4*$10^4$. The magnetic field at the center of the cylinders is $\approx 50\mu$T/1.4*$10^4$ = 3.5*$10^{-9}$ T.

This attenuation was chosen so that the "deflection" of most of the electrons by the magnetic field was within the resolution of the spectrometer. The lateral acceleration can be calculated from the Lorentz force. The electric field will be neglected.

$$F_L = z\overrightarrow{v} \times \overrightarrow{B} = zvBsin\theta \tag{D.4}$$

where $z$ is the charge, $v$ is the velocity, $B$ is the magnetic field, and $\theta$ is the angle between the velocity vector and the electric field. The translation distance $l_x$ or $l_y$ along the x or y axes (i.e., perpendicular to the time of flight axis) can be calculated by considering that an electron will be released with a certain kinetic energy ($E_{kin}$) and direction from which the velocity components can be calculated. The $E_{kin}$ in the determines the velocity, $v(E_{kin}) = \sqrt{\frac{2E_{kin}}{m}}$ and given the length of the time of flight apparatus, L, $t(E_{kin}) = L/v(E_{kin})$.

The radius of the circular path, $R$, can be calculated with the centrifugal force,

$$zvBsin\theta = \frac{mv^2}{R} \Rightarrow R(E_{kin}) = \frac{mv}{zB\sin\theta} \tag{D.5}$$

from which the period of rotation, $T$, can be calculated

$$T(E_{kin}) = \frac{2\pi R(E_{kin})}{v(E_{kin})} = \frac{2\pi m}{zB\sin\theta} \tag{D.6}$$

For a magnetic field of $B = 3.5 * 10^{-9}T$, the period of rotation, $T$, equals 10 ms. This means that a complete cycle is not achieved during the time of flight (order of 1 $\mu$s. For every kinetic energy value, an electron completes $(t(E_{kin})/T(E_{kin}))\, 2\pi R(E_{kin}) =$

0.45 meters of the $2\pi R$ circumference. This corresponds to an arc and is equivalent to $s = 0.45 = R\theta(R(E_{kin}))$ (see Fig. D.1(left) for the definition of the variables). The displacement distance, $l_y$, can be calculated by $R(E_{kin}) - p(E_{kin})$, with

$$\begin{aligned} p(E_{kin}) &= \sqrt{R^2(E_{kin}) - h^2(E_{kin})} \\ &= \sqrt{R^2(E_{kin}) - R^2(E_{kin}) sin^2\theta} \\ &= R(E_{kin}) \cos\theta. \end{aligned} \tag{D.7}$$

Thus, $l_y = R(1-\cos\theta)$. If the electron is released in the z direction (along the time-of-flight axis), and approximate that the z component is perpendicular to the earth's magnetic field the displacement $l_y$ is shown in Fig.D.1(right) . The displacement for electrons emitted with a kinetic energy of 0.18 eV is equivalent to the spatial resolution. For electrons with larger kinetic energy, the displacement is smaller than the resolution of the detector.

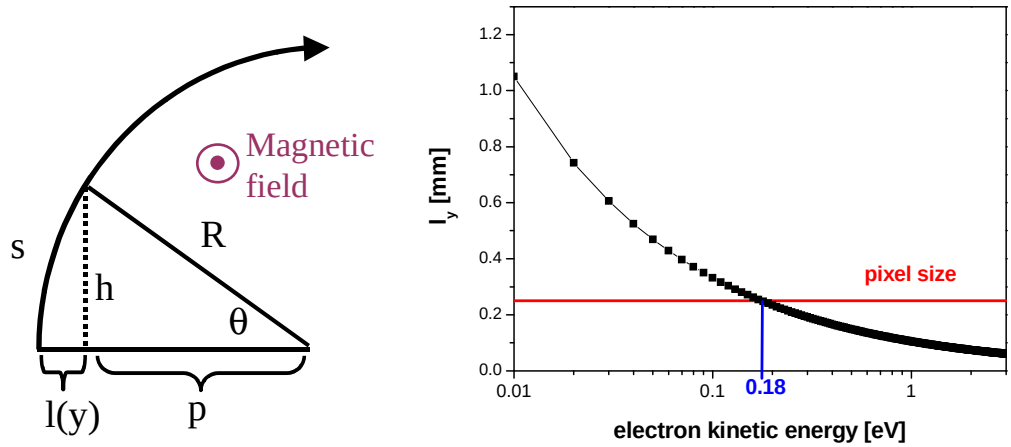


Figure D.1: *The left hand side of the figure shows the Lorentz force definitions for the calculation. The magnetic field propagates out of the page. The right hand side of the figure shows the dependence of the lateral motion as a function of electron kinetic energy.*

The design of the cylinders was intended for an apparatus yet to be built, thus the arrangement of the mu-metal was not optimum for the present apparatus (particularly the gap between the interaction region and vacuum chamber). The two cylinders were open on the detector end, and partially open on the interaction region end. The open ends allow for magnetic fields to penetrate into the center. Fig. D.2 shows a diagram

of the designed mu-metal shielding inside the vacuum chamber. The outer shield was punctuated with several small holes ($\sim$ 50 %) at the position of the ion gauge and vacuum pump as indicated in Fig. D.2. Small holes were chosen over one large hole to reduce the amount of magnetic field penetration.

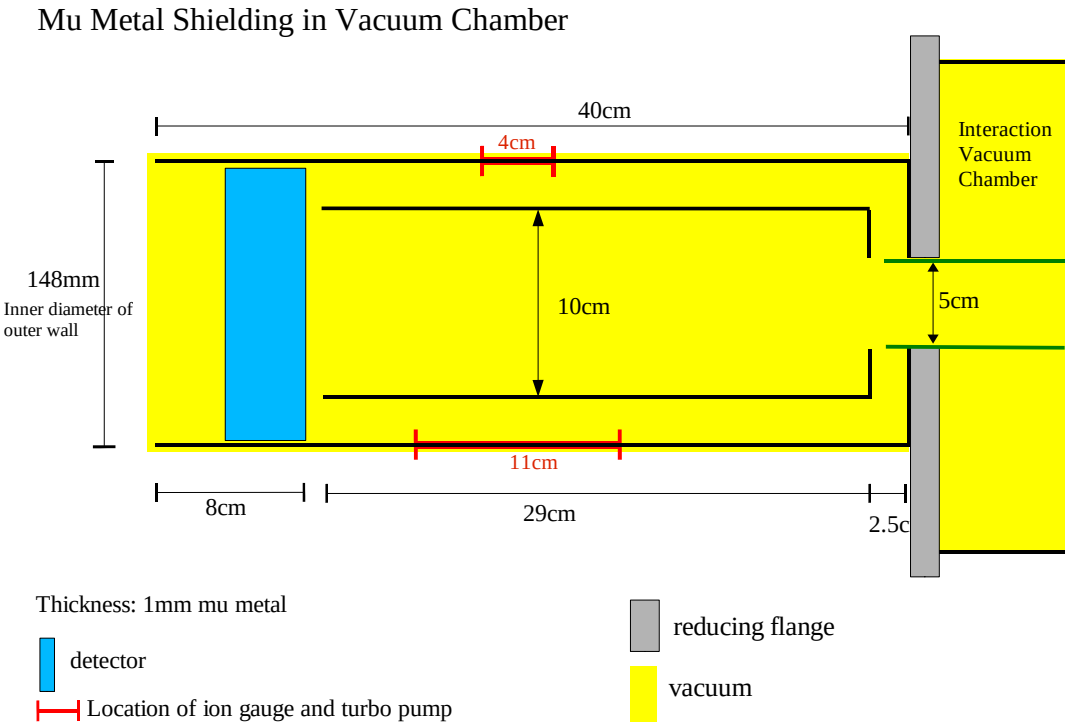


Figure D.2: *Cross section of vacuum apparatus, highlighting the mu-metal scheme. Double walled mu-metal shielding exists only in the new section with the detector. For the outer cylinder, several small holes were placed at the location of the ion gauge and turbo pump. A stop-gap solution was proposed to connect the interaction region with the new chamber.*

From the 5 cm diameter aperture of the new vacuum chamber to the laser interaction region, a single walled cylinder of 5 cm diameter was constructed. Optimally, the double walled cylinder would extend over the interaction region. The solution presented here is only for a temporary adaptation to the present vacuum chamber, and will no longer be used upon construction of the new chamber.